Published for SISSA by Springer

Received: June 29, 2020
Accepted: September 7, 2020
Published: October 7, 2020

Upper limit on the $\eta \to \pi^+\pi^-$ branching fraction with the KLOE experiment

The KLOE-2 collaboration

D. Babusci,[d] M. Berlowski,[v] C. Bloise,[d] F. Bossi,[d] P. Branchini,[s] A. Budano,[r,s] B. Cao,[u] F. Ceradini,[r,s] P. Ciambrone,[d] F. Curciarello,[a,d] E. Czerwiński,[c] G. D'Agostini,[n,o] E. Danè,[d] V. De Leo,[n,o] E. De Lucia,[d] A. De Santis,[d] P. De Simone,[d] A. Di Cicco,[r,s] A. Di Domenico,[n,o] D. Domenici,[d] A. D'Uffizi,[d] A. Fantini,[p,q] P. Fermani,[d] S. Fiore,[t,o] A. Gajos,[c] P. Gauzzi,[n,o] S. Giovannella,[d] E. Graziani,[s] V.L. Ivanov,[g,h] T. Johansson,[u] X. Kang,[w,d,1] D. Kisielewska-Kamińska,[c] E.A. Kozyrev,[g,h] W. Krzemien,[v] A. Kupsc,[u] P.A. Lukin,[g,h] G. Mandaglio,[f,b] M. Martini,[d,m] R. Messi,[p,q] S. Miscetti,[d] D. Moricciani,[d] P. Moskal,[c] S. Parzych,[c] A. Passeri,[s] V. Patera,[l,o] E. Perez del Rio,[n,o] P. Santangelo,[d] M. Schioppa,[j,k] A. Selce,[r,s] M. Silarski,[c] F. Sirghi,[d,e] E.P. Solodov,[g,h] L. Tortora,[s] G. Venanzoni,[i] W. Wiślicki[v] and M. Wolke[u]

[a] *Dipartimento di Fisica e Astronomia "Ettore Majorana", Università di Catania, Italy*
[b] *INFN Sezione di Catania, Catania, Italy*
[c] *Institute of Physics, Jagiellonian University, Cracow, Poland*
[d] *Laboratori Nazionali di Frascati dell'INFN, Frascati, Italy*
[e] *Horia Hulubei National Institute of Physics and Nuclear Engineering, Măgurele, Romania*
[f] *Dipartimento di Scienze Matematiche e Informatiche, Scienze Fisiche e Scienze della Terra dell'Università di Messina, Messina, Italy*
[g] *Budker Institute of Nuclear Physics, Novosibirsk, Russia*
[h] *Novosibirsk State University, Novosibirsk, Russia*
[i] *INFN Sezione di Pisa, Pisa, Italy*
[j] *Dipartimento di Fisica dell'Università della Calabria, Rende, Italy*
[k] *INFN Gruppo collegato di Cosenza, Rende, Italy*
[l] *Dipartimento di Scienze di Base ed Applicate per l'Ingegneria dell'Università "Sapienza", Roma, Italy*
[m] *Dipartimento di Scienze e Tecnologie applicate, Università "Guglielmo Marconi", Roma, Italy*
[n] *Dipartimento di Fisica dell'Università "Sapienza", Roma, Italy*
[o] *INFN Sezione di Roma, Roma, Italy*

[1] Corresponding author.

https://doi.org/10.1007/JHEP10(2020)047

[p] *Dipartimento di Fisica dell'Università "Tor Vergata", Roma, Italy*
[q] *INFN Sezione di Roma Tor Vergata, Roma, Italy*
[r] *Dipartimento di Matematica e Fisica dell'Università "Roma Tre", Roma, Italy*
[s] *INFN Sezione di Roma Tre, Roma, Italy*
[t] *ENEA, Department of Fusion and Technology for Nuclear Safety and Security, Frascati (RM), Italy*
[u] *Department of Physics and Astronomy, Uppsala University, Uppsala, Sweden*
[v] *National Centre for Nuclear Research, Warsaw, Poland*
[w] *School of Mathematics and Physics, China University of Geosciences (Wuhan), Wuhan, China*

E-mail: xiaolin.kang@lnf.infn.it

Abstract: Based on an integrated luminosity of $1.61\,\mathrm{fb}^{-1}$ e^+e^- collision data collected with the KLOE detector at DAΦNE, the Frascati ϕ-factory, a search for the P- and CP-violating decay $\eta \to \pi^+\pi^-$ has been performed. Radiative $\phi \to \eta\gamma$ decay is exploited to access the η mesons. No signal is observed in the $\pi^+\pi^-$ invariant mass spectrum, and the upper limit on the branching fraction at 90% confidence level is determined to be $\mathcal{B}(\eta \to \pi^+\pi^-) < 4.9 \times 10^{-6}$, which is approximately three times smaller than the previous KLOE result. From the combination of these two measurements we get $\mathcal{B}(\eta \to \pi^+\pi^-) < 4.4 \times 10^{-6}$ at 90% confidence level.

Keywords: Branching fraction, CP violation, e^+-e^- Experiments, Rare decay

ArXiv ePrint: 2006.14710

JHEP10(2020)047

Contents

1 Introduction 1

2 The KLOE detector at DAΦNE 2

3 Data sample and event selection 2

4 Upper limit on the branching fraction 5

5 Systematic uncertainty 6

6 Combination with 2001/2002 data 6

1 Introduction

Violation of CP symmetry is a crucial ingredient in understanding the origin of the Baryon Asymmetry in the Universe (BAU). Although the Standard Model (SM) can explicitly accommodate CP violation through a single relevant phase in the Cabibbo-Kobayashi-Maskawa (CKM) quark mixing matrix, this source of CP violation appears largely insufficient to explain the observed value of the BAU.

In the SM the P and CP violating decay $\eta \to \pi^+\pi^-$ can proceed only through CP violating weak interactions via a virtual K^0_S meson, with an expected branching fraction less than 2×10^{-27} [1]. Introducing CP violation in strong interactions through a possible θ-term in the QCD Lagrangian [2] would enhance this limit at the level of $\sim 3 \times 10^{-17}$. Allowing additional CP violation phases in the extended Higgs sector of the electroweak theory could generate the decay with a branching fraction up to 1.2×10^{-15} [3, 4]. By taking into account the higher-order chiral Lagrangian, the couplings of $\eta(\eta')\pi\pi$ can be connected with the neutron electric dipole moment (nEDM) [5]. A recent work using the present upper bound on the nEDM indicates an upper limit for $\eta \to \pi^+\pi^-$ of 5.3×10^{-17} [6].

A branching fraction larger than the above mentioned levels would be an indication of unconventional sources of CP violation, which would possibly help solving the problem of the origin of the BAU, and making the search for the $\eta \to \pi^+\pi^-$ decay worth of experimental investigation at any accessible level at present experimental facilities.

The best upper limit to date on this branching fraction is from the KLOE experiment, $\mathcal{B}(\eta \to \pi^+\pi^-) < 1.3 \times 10^{-5}$ at 90% confidence level (CL) [7], based on the analysis of 350 pb^{-1} of data collected at the ϕ resonance peak in years 2001 and 2002. A recent upper limit has been obtained by the LHCb Collaboration [8], $\mathcal{B}(\eta \to \pi^+\pi^-) < 1.6 \times 10^{-5}$ at 90% CL, searching for the signal in $D^+ \to \pi^+\eta$ and $D^+_s \to \pi^+\eta$ decays produced in proton-proton collisions. The result of a new search for the decay $\eta \to \pi^+\pi^-$ based on an integrated luminosity of 1.61 fb^{-1} of data collected by the KLOE experiment in years 2004 and 2005 is reported in the following, together with its combination with the previous KLOE result.

JHEP10(2020)047

2 The KLOE detector at DAΦNE

DAΦNE [9] is an e^+e^- collider operated at center-of-mass energy of the ϕ meson peak, $\sim$1.020 GeV, with a beam energy spread of (0.302 ± 0.001) MeV. Positron and electron beams collide with a period of 2.7 ns at an angle of $\sim$25 mrad, producing ϕ mesons with a small transverse momentum $\sim$ 13 MeV/c. The longitudinal and horizontal width of the beam-beam collision region is Δz $\sim$12 mm and Δx $\sim$1.2 mm respectively. All these quantities are measured run-by-run to obtain a good precision of the integrated luminosity [10]. The KLOE detector at DAΦNE is composed of a large cylindrical drift chamber (DC) [11] and an electromagnetic calorimeter (EMC) [12] made of lead and scintillating fibres surrounded by a superconducting coil providing a 0.52 T axial magnetic field. The cylindrical drift chamber, 2 m radius and 3.3 m length, is operated with a 90% helium and 10% isobutane gas mixture; its spatial resolution is $\sigma_{xy} \sim 150$ μm and $\sigma_z \sim 2$ mm in the transverse and longitudinal projections, respectively. The transverse-momentum resolution for large-angle tracks is $\sigma_{p_T}/p_T \sim 0.4\%$. Vertices are reconstructed with a spatial resolution of $\sim$ 3 mm. The calorimeter made by lead and scintillating fibers consists of a cylindrical barrel and two end-caps providing a solid angle coverage of $\sim$ 98%. The energy resolution for photons is $\sigma_E/E = 0.057/\sqrt{E(GeV)}$ and the time resolution is $\sigma_t = 54$ ps$/\sqrt{E(GeV)} \oplus 100$ ps. The spatial resolution is 1.4 cm$/\sqrt{E(GeV)}$ along the fibers and 1.3 cm in the orthogonal direction.

The KLOE trigger system [13] uses a two level scheme. The first level trigger is a fast trigger with a minimal delay which starts the acquisition of the EMC front-end-electronics. The second level trigger is based on the energy deposits in the EMC (at least 50 MeV in the barrel and 150 MeV in the end-caps) or on the hit multiplicity information from the DC. The trigger conditions are chosen to minimise the machine background, and recognise Bhabha scattering or cosmic-ray events. Both the calorimeter and drift chamber triggers are used for recording physical events.

The GEANFI Monte Carlo (MC) [14] simulation describes the geometry and material of the KLOE detector, as well as the detector response. Run-by-run machine background conditions are taken into account; the calorimeter energy deposits and drift chamber hits from beam background events triggered at random are overlaid onto the simulated events. The simulated events are processed with the same reconstruction algorithms as the data. The MC production includes all the relevant ϕ decay channels, and continuum processes $e^+e^- \to e^+e^-\gamma$, $\mu^+\mu^-\gamma$, $\pi^+\pi^-\gamma$ to estimate the background contributions. Proper scaling due to the different integrated luminosity of the samples is taken into account when the different MC contributions are merged together. A sample of the signal $\phi \to \eta\gamma$ with $\eta \to \pi^+\pi^-$ is generated to optimise the event selection criteria and to determine the detector efficiency.

3 Data sample and event selection

For the selection of signal candidate events $\phi \to \eta\gamma$ with $\eta \to \pi^+\pi^-$, two opposite charged tracks with a vertex near the e^+e^- interaction point (IP) are required together with an

JHEP10(2020)047

energy deposit (cluster) in the EMC compatible with the photon recoiling against the η meson from the IP. The tracks are reconstructed from hits in drift chamber within the polar angle range $45^\circ < \theta < 135^\circ$. The vertex is required to be within a cylinder, 20 cm long and 8 cm of radius, centered on the IP. To evaluate the time of flight of particles both tracks are required to be associated to a cluster in the EMC. The transverse and three-dimensional distances between the centroid of the associated cluster and the track extrapolation point to the calorimeter front surface are required to be less than 30 cm and 100 cm, respectively (track-to-cluster association). The cluster energy is required to be greater than 10 MeV. If there is more than one cluster satisfying the above requirements, the cluster with the lowest transverse distance is assigned as the associated cluster. The scalar sum of the momenta of the two tracks must lie in the range [0.15,1.03] GeV/c. Selected $\phi \to \rho\pi$ events are used to study the tracking and vertex efficiencies on data and MC. Efficiency corrections as a function of transverse and longitudinal momenta for charged pions reconstruction are applied to all MC samples. The correction for the vertex efficiency is negligible. A background filter algorithm [14] based only on information from the EMC is used to reject cosmic rays and Bhabha scattering background events.

The recoil photon candidate is selected by requiring an isolated energy cluster in the EMC not associated to any track. The condition on cluster time $|T_{cl} - R_{cl}/c| < min(5\sigma_t(E_{cl}), 2ns)$ is used to identify a photon originating from the IP (prompt photon), where T_{cl} is the cluster time, R_{cl} is the distance from the IP, σ_t is the energy-dependent time resolution. To suppress background from $e^+e^- \to \pi^+\pi^-\gamma$ process, the cluster is also required to be at large polar angle $45^\circ < \theta_\gamma < 135^\circ$. As for the two body decay $\phi \to \eta\gamma$ the recoil photon has an energy of 363 MeV in the ϕ rest frame, the selected candidate photon is required to have an energy in the range $[250, 470]$ MeV. To match the missing energy and momentum obtained from the two tracks with the photon kinematics, the angle ψ between the direction of the missing momentum of the two tracks and the direction of the recoil photon, shown in the left panel of figure 1, is required to be less than 0.05 rad.

The remaining background originates from the processes $e^+e^- \to e^+e^-\gamma$, $\mu^+\mu^-\gamma$, $\phi \to \rho^\pm\pi^\mp$ with $\rho^\pm \to \pi^\pm\gamma$, and $\phi \to \pi^+\pi^-\pi^0$ with an undetected photon. To separate $\pi^+\pi^-\gamma$ and $e^+e^-\gamma$ events, particle identification with a time of flight technique is used. The difference between the time of the cluster associated to the track (T_{cl}) and the time calculated from the track length L and particle momentum p under different mass hypotheses is defined as $\delta t_X = T_{cl} - L/(c\beta_X)$, where $\beta_X = p/\sqrt{p^2 + m_X^2}$ and m_X is the pion or electron mass, the scatter plots of δt_e vs δt_π for data and MC simulated signal are shown in figure 2. A track with $0.2 < \delta t_e < 2.5$ ns and $-0.4 < \delta t_\pi < 1.5$ ns is identified as a pion. Events with at least one pion are retained. The cuts have been chosen to optimize the rejection of the $e^+e^-\gamma$ background, while keeping almost unaltered efficiency on the signal.

The $\mu^+\mu^-\gamma$ and $\pi^+\pi^-\pi^0$ background events can be rejected using the mass of the charged tracks, M_{trk}, computed by assuming the ϕ decays to two identical mass particles and a photon, i.e.

$$|\vec{p}_\phi - \vec{p}_1 - \vec{p}_2| = E_\phi - \sqrt{|\vec{p}_1|^2 + M_{trk}^2} - \sqrt{|\vec{p}_2|^2 + M_{trk}^2}, \tag{3.1}$$

where $\vec{p}_\phi$, $\vec{p}_1$ and $\vec{p}_2$ are the three-momentum of ϕ and two charged tracks, respectively;

JHEP10(2020)047

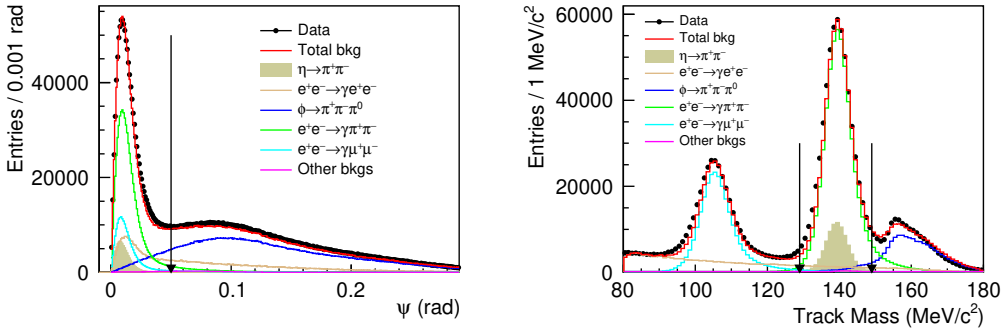

Figure 1. Left: The angle ψ between the direction of missing momentum of $\pi^+\pi^-$ and the prompt photon. Right: Distribution of the mass M_{trk} of the charged-particle tracks. Black dots are data; the red histogram is the sum of all background contributions evaluated from MC simulation: $\phi \to \rho\pi$ with $\rho \to \pi\pi$ (blue histogram), $e^+e^- \to \pi^+\pi^-\gamma$ (green histogram), $e^+e^- \to \mu^+\mu^-\gamma$ (cyan histogram), $e^+e^- \to e^+e^-\gamma$ (yellow histogram), and the sum of other backgrounds (violet histogram). The expected signal is shown as the shaded histogram with the branching fraction of $\eta \to \pi^+\pi^-$ arbitrarily fixed to 8.8×10^{-3} for visualisation purposes.

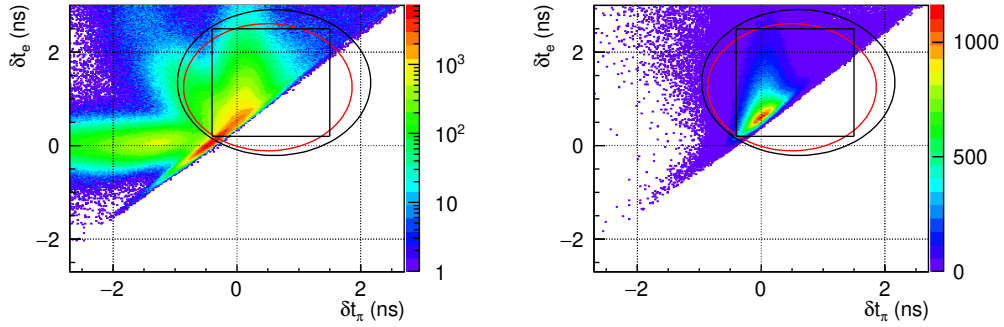

Figure 2. Scatter plot of the time difference for the pion (δt_π) and electron (δt_e) mass hypothesis for data (left) and MC simulated signal (right). Events within the rectangle are retained for further analysis, within the elliptic shapes are for systematic uncertainty studies.

E_ϕ is the energy of the ϕ-meson. Figure 1-right shows the M_{trk} distribution for data, the MC simulated signal and contributions from different background sources. The condition $129 < M_{trk} < 149\,\mathrm{MeV/c^2}$ is required to be fulfilled for candidate events to reject most of the backgrounds from $\mu^+\mu^-\gamma$ and $\pi^+\pi^-\pi^0$.

After the above selection criteria, 59,684 events remain in the η mass region [500,600] MeV/c^2. The $\pi^+\pi^-$ invariant mass spectrum, $M(\pi^+\pi^-)$, is shown as the black dots in figure 3, which will be used to search for the decay $\eta \to \pi^+\pi^-$. The survived events with a $\pi^+\pi^-\gamma$ final state are mainly from $e^+e^- \to \pi^+\pi^-$ accompanied by initial or final state radiation, $\phi \to f_0(980)\gamma$ with $f_0(980) \to \pi^+\pi^-$ and $\phi \to \rho^\pm\pi^\mp$ with $\rho^\pm \to \pi^\pm\gamma$. However, none of these backgrounds is expected to contribute as a peak in the $\pi^+\pi^-$ invariant mass near the η mass value.

The irreducible background in the η signal region [540,555] MeV/c^2 is evaluated by performing a fit to the η side bands, [500,540] and [555,600] MeV/c^2, with a third-order polynomial function. The fit has $\chi^2 = 84.9$ with 81 degrees of freedom; the result is

JHEP10(2020)047

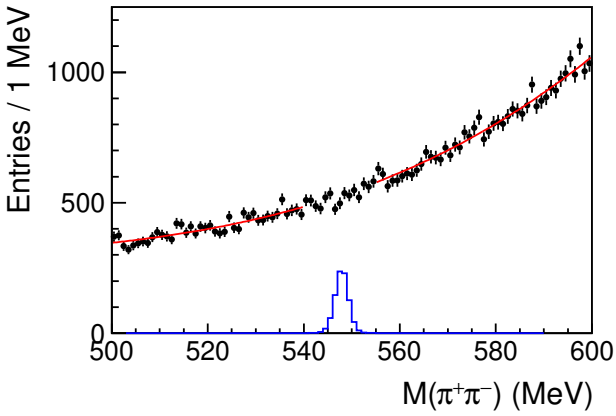

Figure 3. $\pi^+\pi^-$ invariant mass distribution for data taken in 2004/2005. The dots with error bars are data, the red lines represent the fit result to η sidebands, the blue histogram is the η signal with the branching fraction arbitrarily fixed to 8.8×10^{-5} for visualisation purposes.

illustrated by the red lines in figure 3. The η signal is described by the corresponding MC simulated shape, shown as the blue histogram in figure 3; to ease visualisation the signal branching fraction has been arbitrarily fixed to 8.8×10^{-5}.

The $M(\pi^+\pi^-)$ signal shape and resolution are validated comparing the $M(\pi^+\pi^-)$ distributions of data and MC for a pure sample of $K_S \to \pi^+\pi^-$ events.

The detection efficiency for the signal process $\phi \to \eta\gamma$ with $\eta \to \pi^+\pi^-$ is evaluated from MC to be $\varepsilon = (14.70 \pm 0.02_{\rm stat})\%$.

4 Upper limit on the branching fraction

As no evident peak is observed in the distribution of $M(\pi^+\pi^-)$ in the signal region, an upper limit on the branching fraction of $\eta \to \pi^+\pi^-$ is extracted with the CL_s technique [15, 16]. The CL_s value is defined as $p_{s+b}/(1-p_b)$, where p_b is the p-value of the background only hypothesis, p_{s+b} is the p-value of the background plus signal hypothesis. The procedure requires the measured $M(\pi^+\pi^-)$ spectrum, the shape of the estimated background, the η signal shape, and the systematic uncertainties as input [17]; the latter will be described in section 5. It yields as output the limit on the branching fraction $\mathcal{B}(\eta \to \pi^+\pi^-)$, with the number of $\eta \to \pi^+\pi^-$ signal events evaluated as follows:

$$N(\eta \to \pi^+\pi^-) = N_{\eta\gamma} \cdot \mathcal{B}(\eta \to \pi^+\pi^-) \cdot \varepsilon, \tag{4.1}$$

where $N_{\eta\gamma}$ is the number of $\phi \to \eta\gamma$ events with $N_{\eta\gamma} = \mathcal{L}_{\rm int} \cdot \sigma(e^+e^- \to \phi \to \eta\gamma)$; $\mathcal{L}_{\rm int}$ is the integrated luminosity, determined to be $(1.61 \pm 0.01)\,{\rm fb}^{-1}$ from the very large-angle Bhabha scattering events [10]. The cross section $\sigma(e^+e^- \to \phi \to \eta\gamma)$ has been evaluated to be (41.7±0.6) nb and takes into account the small variations of $\sqrt{s}$ on a run by run basis [18].

A series of statistical tests is carried out for each hypothesised $\mathcal{B}(\eta \to \pi^+\pi^-)$ to numerically evaluate the distribution functions for the test statistics. The upper limit on $\mathcal{B}(\eta \to \pi^+\pi^-)$ at 90% CL is determined by requiring the CL_s value equals 0.1 and results

JHEP10(2020)047

to be:

$$\mathcal{B}(\eta \to \pi^+\pi) < 4.9 \times 10^{-6}. \tag{4.2}$$

The corresponding upper limit on the number of signal events is $N(\eta \to \pi^+\pi^-) < 48$.

5 Systematic uncertainty

The systematic uncertainties affecting the $\phi \to \eta(\pi^+\pi^-)\gamma$ analysis mainly originate from the non resonant backgrounds and the difference in variables distributions between data and MC samples.

The estimation of non resonant backgrounds in the signal region by fitting the signal sidebands has a relative uncertainty of 0.5%; by changing the fitting function to second- or fourth-order polynomial or varying the fitting range by $\pm\, 2\,\mathrm{MeV/c^2}$, the result varies within the quoted uncertainty, therefore 0.5% is taken as the systematic uncertainty associated with the non resonant backgrounds.

The systematic uncertainties associated to the selection criteria on ψ and M_{trk} are estimated by varying the cuts within their resolutions respectively and evaluating the corresponding effect on $M(\pi^+\pi^-)$. The relative variation compared to the nominal $M(\pi^+\pi^-)$ spectrum and corrected for the corresponding variation in the MC efficiency is taken as systematic uncertainty, which is determined to be 2.0% for the ψ cut, and 3.0% for the M_{trk} selection.

To evaluate the systematic uncertainty associated with the time of flight selection, the lower cuts of δt_e and δt_π are varied alternatively by $\pm$ 0.1 ns. In addition, different selection criteria adopting elliptic cuts in the (δt_e, δt_π) plane, instead of rectangular, are checked, i.e. $(\delta t_e - 0.6)^2 + (\delta t_\pi - 1.35)^2 < 1.56$ ns^2, or $(\delta t_e - 0.5)^2 + (\delta t_\pi - 1.25)^2 < 1.36$ ns^2, as shown in figure 2. The maximum relative variation compared to the nominal $M(\pi^+\pi^-)$ spectrum and corrected for the corresponding variation in the MC efficiency is found to be around 1.0%, which is taken as systematic uncertainty.

The trigger efficiency has been evaluated from the comparison of the EMC and DC single and coincidence rates. The efficiency is in agreement with the MC evaluation, with a negligible uncertainty.

A sample of non-filtered and non-pre-selected events, prescaled by a factor of 20, is used to validate the efficiency of the background filter and event pre-selection algorithms. The $e^+e^- \to \pi^+\pi^-\gamma$ process is used to estimate the differences between data and MC associated with the two algorithms, the effect is found negligible.

All the systematic uncertainties, including the uncertainty on the integrated luminosity [10] and the cross section $\sigma(e^+e^- \to \phi \to \eta\gamma)$ [18], are listed in table 1, where the total systematic uncertainty is estimated as the sum in quadrature of all contributions.

6 Combination with 2001/2002 data

This section presents the procedure to combine the 2001/2002 data analysed in ref. [7] with the 2004/2005 data sample to get a combined upper limit.

JHEP10(2020)047

Source	Relative uncertainty(%)
Background Estimate	0.5
ψ cut	2.0
M_{trk} cut	3.0
Time of flight cuts	1.0
Integrated luminosity	0.6
$\sigma(e^+e^- \to \phi \to \eta\gamma)$	1.4
Total	4.1

Table 1. Summary of the systematic uncertainties.

In ref. [7] the upper limit was determined at 90% confidence level as:

$$\mathcal{B}(\eta \to \pi^+\pi^-) = \frac{N(\eta \to \pi^+\pi^-)}{N_\eta \cdot \varepsilon} < 1.3 \times 10^{-5}, \tag{6.1}$$

with $N(\eta \to \pi^+\pi^-) < 33$, $\varepsilon = (16.6 \pm 0.2_{\text{stat}} \pm 0.4_{\text{syst}})\%$, and $N_\eta = 1.55 \times 10^7$ the normalisation determined from the observed $\phi \to \eta(3\pi^0)\gamma$ decays with a systematic uncertainty of 2%.

The upper limit for this totally independent data sample has been re-evaluated using the same procedure described in section 4. The signal shape is kept the same as in ref. [7], a Gaussian function centered at the η mass value $M_\eta = 547.874\,\text{MeV}/c^2$ measured by KLOE [19] and a standard deviation of $1.33\,\text{MeV}/c^2$ estimated from the MC simulation. The 90% CL upper limit on $\mathcal{B}(\eta \to \pi^+\pi^-)$ is determined to be 1.36×10^{-5}, which is consistent with the published result.

The procedure described in section 4 is then used to evaluate the upper limit combining the two data samples taking into account their differences in the η signal shape, the observed $M(\pi^+\pi^-)$ spectra and the shape of the estimated backgrounds, similarly to the procedure used in ref. [20]. The systematic uncertainties estimated for both 2001/2002 and 2004/2005 samples are given as input to the procedure. The resulting upper limit at 90% CL is:

$$\mathcal{B}(\eta \to \pi^+\pi^-) < 4.4 \times 10^{-6} \tag{6.2}$$

which is almost a factor of three smaller than the previous limit.

Acknowledgments

We warmly thank our former KLOE colleagues for the access to the data collected during the KLOE data taking campaign. We thank the DAΦNE team for their efforts in maintaining low background running conditions and their collaboration during all data taking. We want to thank our technical staff: G. F. Fortugno and F. Sborzacchi for their dedication in ensuring efficient operation of the KLOE computing facilities; M. Anelli for his continuous attention to the gas system and detector safety; A. Balla, M. Gatta, G. Corradi and G. Papalino for electronics maintenance; C. Piscitelli for his help during major maintenance

JHEP10(2020)047

periods. This work was supported in part by the Polish National Science Centre through the Grants No. 2013/11/B/ST2/04245, 2014/14/E/ST2/00262, 2014/12/S/ST2/00459, 2016/21/N/ST2/01727, 2016/23/N/ST2/01293, 2017/26/M/ST2/00697.

References

[1] C. Jarlskog and E. Shabalin, *How large are the rates of the CP-violating $\eta, \eta' \to \pi\pi$ decays?*, *Phys. Rev. D* **52** (1995) 248 [INSPIRE].

[2] H.-Y. Cheng, *The Strong CP Problem Revisited*, *Phys. Rept.* **158** (1988) 1 [INSPIRE].

[3] C. Jarlskog and E. Shabalin, *On searches for CP, T, CPT and C violation in flavour-changing and flavour-conserving interactions*, *Phys. Scripta T* **99** (2002) 23.

[4] E. Shabalin, *Decays of η and η' mesons caused by the weak interaction*, *Phys. Scripta T* **99** (2002) 104.

[5] T. Gutsche et al., *CP-violating decays of the pseudoscalars η and η' and their connection to the electric dipole moment of the neutron*, *Phys. Rev. D* **95** (2017) 036022 [arXiv:1612.02276] [INSPIRE].

[6] A.S. Zhevlakov, M. Gorchtein, A.N. Hiller Blin, T. Gutsche and V.E. Lyubovitskij, *Bounds on rare decays of η and η' mesons from the neutron EDM*, *Phys. Rev. D* **99** (2019) 031703 [arXiv:1812.00171] [INSPIRE].

[7] KLOE collaboration, *Upper limit on the $\eta \to \pi^+\pi^-$ branching ratio with the KLOE detector*, *Phys. Lett. B* **606** (2005) 276 [hep-ex/0411030] [INSPIRE].

[8] LHCb collaboration, *Search for the CP-violating strong decays $\eta \to \pi^+\pi^-$ and $\eta'(958) \to \pi^+\pi^-$*, *Phys. Lett. B* **764** (2017) 233 [arXiv:1610.03666] [INSPIRE].

[9] A. Gallo et al., *DAΦNE status report*, *Conf. Proc. C* **060626** (2006) 604 [INSPIRE].

[10] KLOE collaboration, *Measurement of the DAΦNE luminosity with the KLOE detector using large angle Bhabha scattering*, *Eur. Phys. J. C* **47** (2006) 589 [hep-ex/0604048] [INSPIRE].

[11] M. Adinolfi et al., *The tracking detector of the KLOE experiment*, *Nucl. Instrum. Meth. A* **488** (2002) 51 [INSPIRE].

[12] M. Adinolfi et al., *The KLOE electromagnetic calorimeter*, *Nucl. Instrum. Meth. A* **482** (2002) 364 [INSPIRE].

[13] KLOE collaboration, *The trigger system of the KLOE experiment*, *Nucl. Instrum. Meth. A* **492** (2002) 134 [INSPIRE].

[14] F. Ambrosino et al., *Data handling, reconstruction, and simulation for the KLOE experiment*, *Nucl. Instrum. Meth. A* **534** (2004) 403 [physics/0404100] [INSPIRE].

[15] A. Birnbaum, *On the foundations of statistical inference*, *J. Am. Statist. Assoc.* **57** (1962) 269.

[16] A.L. Read, *Presentation of search results: The CL(s) technique*, *J. Phys. G* **28** (2002) 2693 [INSPIRE].

JHEP10(2020)047

[17] T. Junk, *Confidence level computation for combining searches with small statistics*, *Nucl. Instrum. Meth. A* **434** (1999) 435 [hep-ex/9902006] [INSPIRE].

[18] S. Giovannella and S. Miscetti, *Study of the $e^+e^- \to \pi^0\pi^0\gamma$ process using 2001/2002 data*, KLOE note 212, http://www.lnf.infn.it/kloe/pub/knote/kn212.ps, (2006).

[19] KLOE collaboration, *Precise measurements of the eta and the neutral kaon meson masses with the KLOE detector*, *JHEP* **12** (2007) 073 [arXiv:0710.5892] [INSPIRE].

[20] KLOE-2 collaboration, *Combined limit on the production of a light gauge boson decaying into $\mu^+\mu^-$ and $\pi^+\pi^-$*, *Phys. Lett. B* **784** (2018) 336 [arXiv:1807.02691] [INSPIRE].

JHEP10(2020)047